Simple Vehicle Powertrain Model for Modeling Intelligent Vehicle Applications

Hesham A. Rakha, *Member, IEEE*, Kyoungho Ahn, Waleed Faris, and Kevin S. Moran

***Abstract*—This research develops a simple vehicle powertrain model that can be incorporated within microscopic traffic simulation software for the modeling of intelligent vehicle applications. This simple model can be calibrated using vehicle parameters that are publically available without the need for field data collection. The model uses the driver throttle level input to compute the engine speed and, subsequently, the engine torque and power to finally compute the vehicle acceleration, speed, and position. The model is tested using field measurements and is demonstrated to produce vehicle power, fuel consumption, acceleration, speed, and position estimates that are consistent with field observations.**

***Index Terms*—Emission, energy management, traffic modeling, vehicles, velocity control.**

I. Introduction

THE RESEARCH presented in this paper develops a vehicle powertrain model that can be integrated with traffic simulation software and vehicle fuel consumption and emission models. Many publications have been written on the modeling of vehicle engines and controls [1]–[8]. Specifically, these models were developed with a focus on engine design, analysis, and control. While these models suffice for their intended purposes, they are not adequate for use in microscopic traffic simulation software for two reasons. Ni and Henclewood [9] indicated that typical engine models are computationally intensive and cannot be integrated within car-following, lane-changing, and gap acceptance algorithms, which are critical components of traffic simulation models. Second, these models require proprietary parameters that are difficult to obtain and, in some instances, require gathering field data for the entire envelope of operation of a vehicle. Thus, the development of a vehicle powertrain model that can be utilized in traffic simulation software is a new challenge for traffic engineers.

The task of driving an automobile is a demanding task, given that drivers must perform lateral-directional loop closure, longitudinal loop closure, information gathering, and hazard detection. In the case of lateral-directional loop closure, drivers use the steering wheel to control lane position and heading. Alternatively, in the case of longitudinal loop closure, drivers use the accelerator and brake pedal, as well as the gear shift lever and clutch in manual transmission vehicles, to control the vehicle's longitudinal position and speed. At the same time, drivers must attend to additional in-vehicle tasks associated with the instrument panel and related comfort/convenience items.

Microscopic traffic simulation software use car-following models to capture the longitudinal motion of a vehicle and its interaction with the preceding vehicle traveling in the same lane [10], [11]. The first equation characterizes the motion of the following vehicle (FV) with respect to the behavior of the lead vehicle (LV). The second set of equations constrains the car-following behavior by ensuring that vehicle accelerations are realistic. The model can be presented by either characterizing a relationship between a vehicles' desired speed and the vehicle spacing (speed formulation) or, alternatively, describing a relationship between the vehicle's acceleration and speed differential between the FV and LV (acceleration formulation). The latter formulation is typical of the well-known General Motors car-following models with a control variable (acceleration), a stimulus variable (speed differential), and a driver sensitivity parameter. Rakha *et al.* [10] demonstrated that the speed formulation is a more appropriate formulation.

To ensure feasible vehicle accelerations, one may consider a vehicle kinematics model, a constant power vehicle dynamics model [12], a variable power vehicle dynamics model [13], or a more sophisticated gear-shifting model. A vehicle dynamics or gear-shifting modeling approach is better because the model parameters can be adjusted to reflect different weather, tire, and roadway surface conditions without the need to gather field data.

The research presented in this paper enhances vehicle longitudinal motion modeling by developing a simple vehicle powertrain model that can be easily implemented within traffic simulation software and can be integrated with power-based vehicle fuel consumption and emission models. A key input to the powertrain model is the driver throttle input. Driver throttle input is a key parameter to modeling different levels of driver aggressiveness to represent real-world driving conditions in traffic simulation models. The proposed model utilizes the throttle level as a key input variable to characterize the driving behavior on roadways. Intra- and interdriver variability is likely present, depending on the surrounding traffic conditions and the driver's psychological state (e.g., fatigued, in a rush, or distracted). This paper, however, focuses on the modeling of

Manuscript received October 28, 2010; revised May 19, 2011 and October 21, 2011; accepted December 3, 2011. Date of publication March 24, 2012; date of current version May 30, 2012. The Associate Editor for this paper was B. De Schutter.

H. A. Rakha and K. Ahn are with the Center for Sustainable Mobility, Virginia Tech Transportation Institute, Blacksburg, VA 24061 USA (e-mail: hrakha@vt.edu).

W. Faris is with the Department of Mechanical Engineering, International Islamic University Malaysia, Gombak Campus, Kuala Lumpur 53100, Malaysia.

K. S. Moran is with Advanced Driver Assistance Systems, NAVTEQ Corporation, Chicago, IL 60606 USA.

Color versions of one or more of the figures in this paper are available online at http://ieeexplore.ieee.org.

Digital Object Identifier 10.1109/TITS.2012.2188517

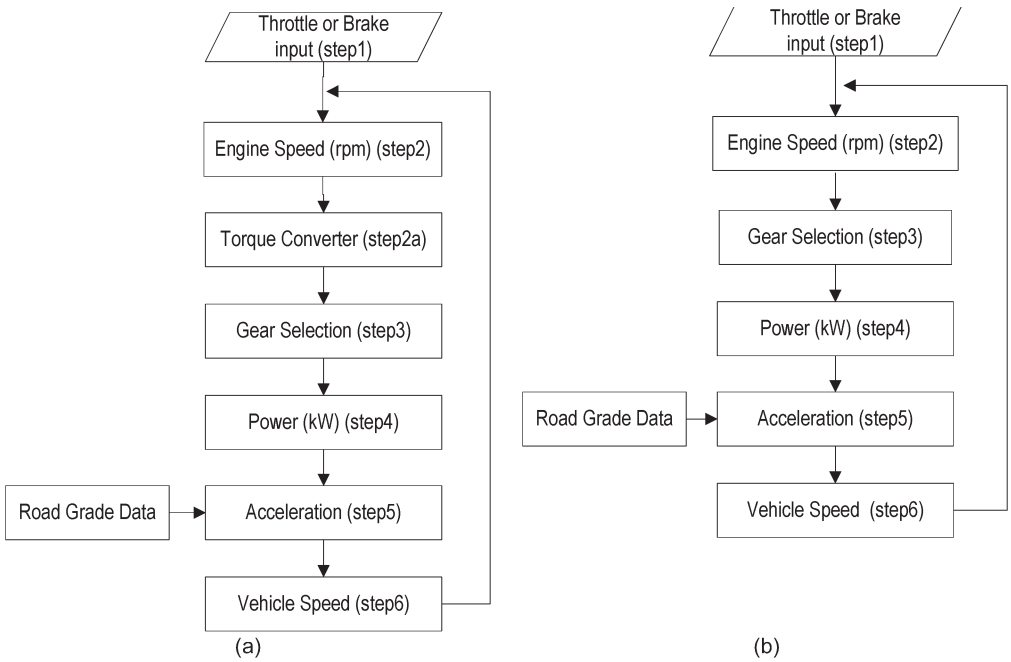

Fig. 1. Proposed model structure. (a) Automatic transmission. (b) Manual transmission.

a vehicle powertrain system, assuming that the driver input is known. Research is currently underway to characterize driver throttle input, depending on the vehicle, roadway, and surrounding traffic conditions.

In terms of the paper layout, initially, the proposed model is described. Subsequently, a description of the field tests and data that were gathered for model testing are presented. The model testing results are presented, followed by the conclusions of the study and recommendations for further research.

II. Model Description

The model starts with the driver throttle and brake pedal input, as shown in Fig. 1 (step 1). Based on the driver's throttle input (f_t), the engine speed (ω_e) is computed using a simple regression model [step 2 or (1)] that was empirically developed as part of this research effort. In the case of a manual transmission system, gear selection (step 3 or *gear selection modeling*) is made directly using the engine speed. Alternatively, in the case of an automatic transmission system, the torque converter (step 2a or *torque converter modeling*) is modeled as shown in Fig. 1. In particular, the torque converter calculates the torque converter output speed and torque, and selects the appropriate gear. Subsequently, the engine speed is used to estimate vehicle torque and power [step 4 or (7)]. The engine power and torque are computed considering an upper bound parabolic function that was proposed by Ni and Henclewood [9] $(P_{\max}(\omega))$. The actual power available is estimated as the proportion of the maximum power considering a linear relationship between the throttle position and the proportion of the maximum power available (i.e., $P(\omega) = f_p \times P_{\max}(\omega)$). The vehicle acceleration [step 5 or (11)] is then computed considering a point mass vehicle dynamics model. The vehicle speed and position [step 6 or (15)] are estimated by solving a second-order differential equation. The specifics of each of the components of the model are described in the succeeding sections.

The model assumes that the powertrain is stiff and the transmission is modeled considering a gear ratio and efficiency. The model makes the following simplifying assumptions:

1) The clutch is assumed to be stiff (i.e., the torque and angular speed remain the same before and after the clutch).
2) Transmission inertia is disregarded (i.e., the model only considers a conversion ratio and efficiency of the transmission system).
3) The propeller shaft is assumed to be stiff.
4) The final powertrain is modeled considering the efficiency.
5) The drive shafts are assumed to be stiff.

Consequently, the overall efficiency is computed as power losses in the engine due to internal friction and other factors, whereas the overall gear ratio is computed as the product of the transmission and final gear ratios.

A. Throttle/Engine Speed Modeling

As was mentioned earlier, the task of driving an automobile is demanding, given that drivers must perform lateral-directional loop closure, longitudinal loop closure, information gathering, and hazard detection. In the case of longitudinal loop closure, drivers use the accelerator and brake pedal, as well as the gear shift lever and clutch in manual transmission vehicles, to control the longitudinal position and speed of the vehicle. At the same time, drivers must attend to additional in-vehicle tasks associated with the instrument panel and related comfort/convenience items. The driver accelerator pedal input in turn affects the throttle level of the vehicle engine. The modeling of driver input entails modeling the driver accelerator pedal level and its effect on the throttle level. This two-level

process can be modeled using a single model without the need to capture the accelerator pedal position. The advantage of the latter approach is that data can be gathered using onboard diagnostic (OBD) readers without the need for cameras to capture the accelerator pedal position. This approach is used in this study.

The driver selected throttle level results in a change in the engine speed and torque. In an attempt to establish a relationship between throttle level $(f_t(t))$ and engine speed $(\omega_e(t))$ at any instant t, field data were gathered using a 1999 Ford Crown Victoria. The vehicle was powered by a 4.6-L V-8 engine using an 87-octane fuel and rated at 200 hp at 4250 rev/min, with an electronic four-speed automatic overdrive transmission. The vehicle, which was owned by the Virginia Tech Transportation Institute (VTTI), had a mileage of 9500 mi at the start of the tests. An OBD reader was used to gather the driver input and engine speed. The data were gathered for typical driving along the Route 460 Bypass and Main Street in Blacksburg. The 460 Bypass is a 7-km limited-access divided highway between Christiansburg, VA, and Blacksburg, VA, whereas Main Street is a signalized arterial. A total of 13 trip repetitions were made to ensure that sufficient data were available. The data were then sorted and binned based on the throttle level. The average engine speed within each throttle level bin was then computed, and a relationship between throttle level and engine speed was derived, as shown in Fig. 2. A least-square-error regression was applied to the data, considering the throttle level as the response variable and the engine speed as the explanatory variable. The calibrated model, which has a high coefficient of determination $(R^2 = 0.92)$, is of the form

$$\omega_e(t) = (\omega_t - \omega_{\text{idle}}) \frac{\ln(f_t(t)) - \ln(f_{\min})}{\ln(f_{\max}) - \ln(f_{\min})} + \omega_{\text{idle}} \quad (1)$$

where $\omega_e(t)$ is the engine speed (in revolutions per minute) at any instant t; ω_t is the engine speed at maximum torque (in revolutions per minute); ω_{idle} is the idling engine speed (in revolutions per minute); $f_t(t)$ is the throttle position at any instant t $[f_{\min}, f_{\max}]$; $f_{\min}$ is the minimum throttle position (in percent); and $f_{\max}$ is the maximum throttle position (in percent). The model requires the calibration of four vehicle specific parameters, i.e., the engine idling speed, the engine speed at maximum power, the minimum throttle level, and the maximum throttle level. The first two parameters can be easily obtained from auto manufacturer websites, whereas the latter two parameters can either be obtained by gathering engine data using an OBD reader or assumed to be approximately 10%–15% and 90%–100%, respectively. The field gathered data demonstrated that the throttle level ranges between 15% and 65% under typical normal driving conditions.

The percentage of maximum power $(f_p(t))$ used at any instant t is then computed considering a linear transformation from the throttle level $f_t(t)$ $[f_{\min}, f_{\max}]$ as

$$f_p(t) = \frac{1}{(f_{\max} - f_{\min})} \left[\left(1 - \frac{f_{\min}}{100}\right) f_t(t) - \left(1 - \frac{f_{\max}}{100}\right) f_{\min} \right]. \quad (2)$$

The proportion of power available at any instant t ranges between $f_{\min}$ and 1.0. The power estimate is comparable to what other researchers have observed from empirical data [14]. The empirical data demonstrated that the fuel consumption $(\delta(\omega_e))$ can be computed as the product of the proportion of pedal signal $(P \in [0, 1])$ and the maximum fuel consumption rate as [14]

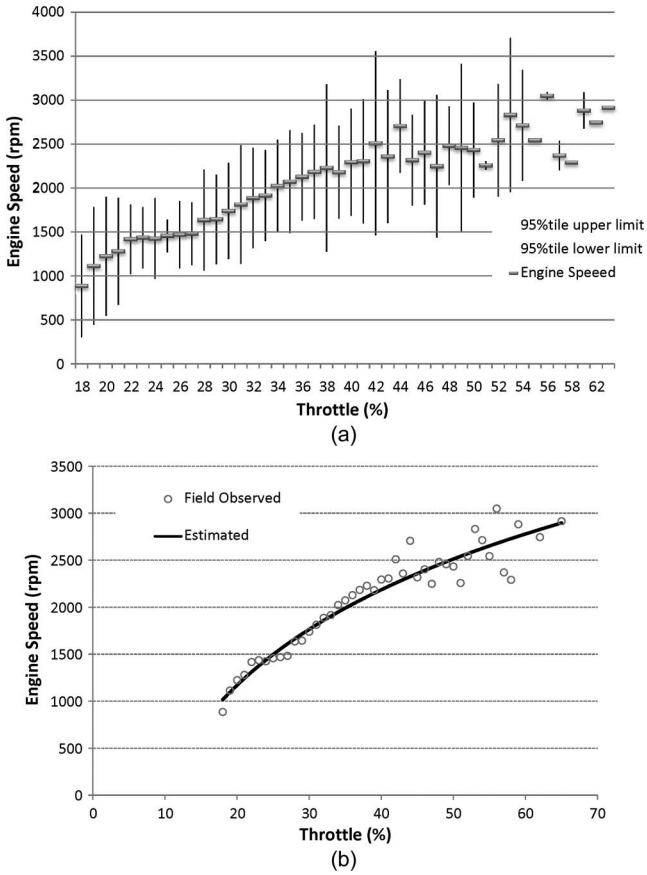

Fig. 2. Example throttle versus engine speed relationship. (a) Field mean and 95% confidence limits. (b) Model predictions versus field observations.

$$\delta(\omega_e) = P \cdot \widehat{\delta}_{\max}(\omega_e). \quad (3)$$

Consequently, it is reasonable to assume for the proportion of power available to equal the product of the maximum power envelope, which is described in the following section, and the throttle signal as

$$P(\omega(t)) = f_p(t) \times P_e(\omega_e(t)). \quad (4)$$

Here, $P(\omega(t))$ is the available engine power at engine speed $\omega_e(t)$, and $P_e(\omega(t))$ is the maximum engine power at engine speed $\omega_e(t)$ and is computed using (7), as will be described later.

It should be noted that, while additional empirical engine data are required to characterize the functional relationship between the throttle level and the engine speed for different vehicle types, engine sizes, engine technologies, and vehicle age/mileage, the validation of the model presented later in this paper indicates that the model produces a good match to field measurements.

B. Engine Modeling

Although there has been a wealth of literature published on the modeling of internal combustion engines, these models were developed with a focus on engine design, analysis, and control [9]. While these models are sufficient for their intended purposes, they are not adequate for use in traffic simulation software for two reasons: First, they are computationally intensive and cannot be integrated within car-following, lane-changing, and gap acceptance algorithms. Second, these models require proprietary parameters that are difficult to obtain and, in some instances, require gathering field data for the entire envelope of operation of a vehicle. Ni and Henclewood [9] summarized the desired attributes of such a model.

1) Accuracy: The engine model must provide reasonable accuracy to predict engine performance with throttle and engine speed as inputs and engine power and torque as outputs. In this paper, we define accuracy as providing a good approximation for the engine behavior with good repeatability for different engines.
2) Computational efficiency: The engine model must be simple enough to facilitate onboard computing with high frequency in real time.
3) Accessibility: To assist wide deployment across different vehicle platforms, the engine model should not rely on proprietary parameters and variables that are difficult to measure. All the information needed to run the model should be publicly available.
4) Formulation: The engine model should be analytical. Engine models based on lookup tables are not only prohibitive to prepare for each individual vehicle but also resource demanding in computation.
5) Calibration: The engine model should be simple to ensure that the model calibration is simple and easy.

Ni and Henclewood [9] presented three simple engine models. The first of these models is a polynomial model that was developed by Genta [15]. This model uses a polynomial to empirically approximate the relationship between engine power P_e (in kilowatts) and engine speed ω_e (in revolutions per minute) as [15]

$$P_e = \sum_{i=1}^{3} C_i \omega_e^i \tag{5}$$

where C_i, $i = 0, 1, 2, 3$, are coefficients and can be estimated from empirical engine curves. These coefficients can be estimated as [16]

$$C_1 = \frac{P_{\max}}{\omega_p} \quad C_2 = \frac{P_{\max}}{\omega_p^2} \quad C_3 = -\frac{P_{\max}}{\omega_p^3} \tag{6}$$

where $P_{\max}$ (in kilowatts) is the peak power, and ω_p (in revolutions per minute) is the engine speed at peak power.

The second model that was developed by Ni and Henclewood assumes a parabolic relationship between the engine torque T_e (in Newton-meter) and engine speed ω_e (in revolutions per minute). Using this assumption, the relationship between the maximum engine power and speed can be written as [9]

$$P_e(\omega_e) = \frac{P_{\max}}{2\omega_p^2}(3\omega_p - \omega_t)\omega_e - \frac{P_{\max}}{2\omega_p^2(\omega_p - \omega_t)}(\omega_e - \omega_t)^2\omega_e \tag{7}$$

where ω_t is the engine speed at peak torque (in revolutions per minute). The engine torque T_e (in Newton-meter) can be computed as [7]

$$T_e = 60000\frac{P_e}{2\pi\omega_e}. \tag{8}$$

The final model developed by Ni and Henclewood [9] is based on Bernoulli's principle. Because this model is more complicated than the other two models, the model equation is not presented here. The interested reader can refer to Ni and Henclewood's paper for more detailed information [9].

Ni and Henclewood validated the three models using empirical curves for four automotive engines: a 2008 Mercedes CLS, a 2006 Honda Civic, a 2006 Pagani Zonda, and a 1964 Chevrolet Corvair. The study concluded that, in terms of computational efficiency, the three models are all acceptable with the polynomial and parabolic models being particularly efficient. In terms of accessibility, the polynomial and parabolic models were found to be excellent because they do not require any proprietary parameters or difficult-to-measure variables. All the three models were equally good in terms of analytical formulation. Given that the Bernoulli model requires much effort to calibrate whereas the other two models involve minimal calibration effort, Ni and Henclewood did not recommend the use of the Bernoulli model. Ni and Henclewood concluded that the parabolic model appeared to be the best among the three models when all evaluation criteria were considered. Consequently, the proposed framework uses the parabolic model that is presented in (7) to establish the vehicle engine power envelope. Depending on the throttle level, the available power is reduced using (2).

C. Torque Converter Modeling

As was mentioned earlier, automatic transmission passenger car vehicles in North America are typically equipped with a torque converter. Wong [17] indicated that a "*torque converter consists of at least three rotary elements known as the pump (impeller), the turbine, and the reactor*." Wong [17] also mentioned that "*the pump is connected to the engine shaft, and the turbine is connected to the output shaft of the converter, which in turn is coupled with the input shift of the multispeed gearbox. The reactor is coupled to an external casing to provide a reaction on the fluid circulating in the converter. The function of the reactor is to enable the turbine to develop an output torque higher than the input torque of the converter, thus to obtain a torque multiplication. The reactor is usually mounted on a free wheel (one-way clutch) so that when the starting period has been completed and the turbine speed is approaching that of the pump, the reactor is in free rotation. At this point, the converter operates as a fluid coupling, with a ratio of output*

torque to input torque equal to 1.0." Wong [17] summarized the advantages of a torque converter.

1) When properly matched, it will not stall the engine.
2) It provides a flexible coupling between the engine and the driven wheels (or sprockets).
3) Together with a suitably selected multispeed gearbox, it provides torque-speed characteristics that approach the ideal.

The performance characteristics of a torque converter are usually described in terms of four parameters: 1) the speed ratio $C_{\rm sr}$, which is the ratio of the output to input speed; 2) the torque ratio $C_{\rm tr}$, which is the ratio of the output to input torque; 3) the efficiency η_c, where $\eta_c = C_{\rm sr}C_{\rm tr}$; and 4) the capacity factor $K_{\rm tc} = \text{speed}/(\text{torque})^{0.5}$.

The torque converter was modeled here.

1) The capacity factor is computed as $K_{\rm tc} = K_e = \omega_e/\sqrt{T_e}$, where ω_e is the engine (input) speed and T_e is the engine (input) torque. The engine speed is computed using (1), and the engine torque is computed using (7) and (8).
2) The speed ratio $(C_{\rm sr})$ is computed from the relationship between $K_{\rm tc}$ and $C_{\rm sr}$. This relationship is derived from curves in the literature [17].
3) The torque converter speed and torque ratios are computed using the relationships between $C_{\rm sr}$ and $C_{\rm tr}$ and between $C_{\rm sr}$ and η_c, respectively. Again, these relationships were derived from the literature [17].
4) The torque converter output speed $(\omega_{\rm tc})$ and torque $(T_{\rm tc})$ are computed as $\omega_{\rm tc} = C_{\rm sr}\omega_e$ and $T_{\rm tc} = C_{\rm tr}T_e$, respectively.
5) The power leaving the torque converter $(P_{\rm tc})$ is computed as $P_{\rm tc} = (2\pi T_{\rm tc}\omega_{\rm tc}/60000)$.

D. Gear Selection Modeling

Once the powertrain speed is computed, the next step is to evaluate the need to shift gears through the modeling of a transmission system. Wong [17] indicated that "*the term 'transmission' includes all of those systems or subsystems employed for transmitting the engine power to the driven wheels or sprockets. There are two common types of transmission for road vehicles: the manual gear transmission, and the automatic transmission with a torque converter. Other types of transmissions, such as continuous variable transmission (CVT) and hydrostatic transmission, are also in use.*"

Wong [17] indicated that the principal requirements for the transmission are given as follows: 1) to achieve the desired maximum speed with an appropriate engine; 2) to be able to start, fully loaded, in both forward and reverse directions on a steep gradient, which is typically 33%; and 3) to properly match the characteristics of the engine to achieve the desired operating fuel economy and acceleration characteristics.

A manual gear transmission usually consists of a clutch, a gearbox, a propeller shaft, and a drive axle with a differential (to allow relative rotation of the driven tires during turning maneuvers). The gearbox provides a number of gear reduction ratios ranging from three to five for passenger cars and 5 to 16 or more for commercial vehicles. The number of gear ratios is selected to provide the vehicle with the propulsive effort-speed characteristics as close to the ideal as possible in a cost-effective manner. The gear ratio for the highest gear is computed as [17]

$$\xi_n = \frac{n_{e1} r (1-i)}{v_{\max} \xi_{\rm ax}} \tag{9}$$

where ξ_n is the gear ratio of the highest gear in the gearbox for an n-speed vehicle, n_{e1} is the engine speed corresponding the maximum speed (which is about 10% higher than the speed at maximum power), r is the rolling radius of the tire, i is the tire slip (2%–5%), $v_{\max}$ is the maximum desired speed, and $\xi_{\rm ax}$ is the gear ratio in the drive axle.

The lowest gear ratio is computed so that a vehicle can accelerate on a grade at a desired acceleration rate. The formula for computing this gear ratio varies depending on whether the vehicle is forward- versus rear-wheel drive. Once the highest and lowest gear ratios are determined, the remaining gear ratios are selected to establish the following relationship [17]:

$$\frac{\xi_2}{\xi_1} = \frac{\xi_3}{\xi_2} = \cdots = \frac{\xi_n}{\xi_{n-1}} = K_g \tag{10}$$

where $K_g = \sqrt[n-1]{\xi_n/\xi_1}$.

Gear shifting is typically controlled by shift maps that provide electronic shift points. The gear control is typically governed by various factors that include the following: 1) the engine speed; 2) the throttle position; 3) the pedal position; and 4) the vehicle speed. The proposed model uses a simple algorithm that is solely based on the engine speed in shifting gears. The model assumes that drivers or the transmission system makes gear shifts when the vehicle reaches the engine speed at peak torque ω_t. Downshifts are made when the vehicle reaches an engine speed of 1500 rev/min based on typical values provided in the literature (1000–2000 rev/min).

E. Vehicle Acceleration Modeling

Once the power generated by the powertrain is computed, the vehicle acceleration at any instant t, i.e., $a(t)$, can be estimated as

$$a(t) = \left[\frac{F(t) - R(t)}{m\,(1.04 + 0.0025\xi_0(t)^2)}\right] \tag{11}$$

where $F(t)$ is the vehicle propulsive force at instant t (in Newtons), $R(t)$ is the sum of resistance forces at instant t acting on the vehicle (in Newtons), m is the vehicle mass (in kilograms), and $\xi_0(t)$ is the final gear ratio at instant t. The powertrain propulsive force is computed as the minimum of the engine or torque converter propulsive force and the maximum frictional force that can be sustained between the vehicle's wheels on the propulsive axle and the roadway surface as

$$F(t) = \min\left[3600 \cdot \eta_d \cdot \frac{f_p(t) P_{\max}(\omega_e)}{v(t)}, 9.81 \cdot m_{\rm ta} \cdot \mu\right] \tag{12}$$

where η_d is the efficiency, $P_{\max}(\omega_e)$ is the maximum propulsive power at the specific engine speed (equal to P_e for manual transmission or $P_{\rm tc}$ for automatic transmission), v is the vehicle speed one time step earlier (in kilometers per hour); $m_{\rm ta}$ is

the mass on the propulsive axle (in kilograms); and μ is the coefficient of roadway adhesion.

The resultant resistance force acting on the vehicle at any instant t is computed as the sum of the aerodynamic, the rolling, and the grade resistance forces. The first resistance force is the aerodynamic resistance that varies as a function of the square of the air speed. Although a precise description of the various forces would involve the use of vectors, for most transportation applications, scalar equations suffice if the forces are considered to only apply in the roadway longitudinal direction. The second resistance force is the rolling resistance, which is a linear function of the vehicle speed and mass. The final resistance force is the grade resistance force, which is a function of the vehicle mass and roadway grade at instant t, $G(t)$. Using the three resistance forces, the resultant resistance force can be computed as [7]

$$R(t) = \frac{\rho}{25.92} C_D C_h A_f v^2(t) + 9.81 m C_r \left[c_5 v(t) + c_6\right] + 9.81 m G(t) \quad (13)$$

where ρ is the density of air at sea level and a temperature of 15 °C (59 °F) (equal to 1.2256 kg/m^3); C_D is the drag coefficient (unitless); C_h is a correction factor for altitude (unitless); A is the vehicle frontal area (m^2); and C_r, c_5, and c_6 are rolling resistance parameters that vary as a function of the road surface type, condition, and vehicle tires, respectively [18]. Generally, radial tires provide a resistance that is 25% less than that for bias ply tires.

Given that the air density varies as a function of altitude H (m), the C_h factor can be computed as

$$C_h = 1 - 8.5 \times 10^{-5} H. \quad (14)$$

Typical values of vehicle frontal areas for different vehicle types and typical drag coefficients are provided in the literature [18]. Similarly, typical values for the coefficient of roadway adhesion and the rolling resistance coefficients are provided in the literature [13], [18].

Once the acceleration is computed, the vehicle speed and position can then be computed by solving the following equations:

$$v(t + \Delta t) = v(t) + a(t)\Delta t$$
$$x(t + \Delta t) = x(t) + v(t)\Delta t + \frac{1}{2} a(t)(\Delta t)^2. \quad (15)$$

Finally, the engine speed can be computed, assuming minimum slippage, as

$$\omega_e(t + \Delta t) = \min\left(\max\left(\frac{1000 v(t + \Delta t)\xi_0}{120\pi r(1 - i)}, \omega_{\text{idle}}\right), \omega_{\text{red}}\right) \quad (16)$$

where ω_{red} is the redline or maximum engine speed. This parameter can be easily obtained from automotive websites. The model also utilizes a maximum comfortable deceleration level. While the deceleration level is a function of the roadway surface condition, the type of vehicle tires, the type of vehicle braking system (ABS), and the driver input, the proposed study utilizes a fixed deceleration level for the simplified model.

III. Model Testing I

The testing of the proposed powertrain model was conducted using data gathered earlier along the Smart Road test facility at Virginia Tech [12], [13]. In addition to documenting all available information on the vehicle and roadway characteristics, the data were gathered under conditions in which vehicle accelerations were not constrained by surrounding traffic. Furthermore, the drivers accelerated at the maximum possible acceleration level, and thus, the $f(t)$ parameter was calibrated while assuming it to be constant. Unfortunately, because the data were gathered using a Global Positioning System (GPS) unit, the driver throttle input was not available and thus had to be computed. This section summarizes the key parameters associated with the test facility, the test vehicles, and the data collection procedures.

A. Test Facility

Testing of vehicles was performed on a 1.6-km (1-mi) section of the Smart Road test facility at the VTTI in Blacksburg, VA. The selected test section featured a relatively straight horizontal layout with a minor horizontal curvature that had no effect on vehicle speeds, a good asphalt roadway surface, and a substantial upgrade that ranged from 6% at one end to 2.8% at the other end. Since no flat sections of significant length were available, vehicle accelerations were measured by driving vehicles uphill.

An equation characterizing the grade of the test section was derived from the elevations of 15 stations along the test section. The vertical profile of the test section was then generated by interpolating between station elevations using a cubic spline interpolation procedure at 1-m (3.28-ft) increments. The cubic spline interpolation ensured that the elevations, slopes, and slope rate of change were identical at the boundary conditions (in this case, every meter). The grade was then computed for each 1-m section (3.28-ft), and a polynomial regression model was fit to the grade data (R^2 of 0.951) to ensure a smooth transition in the roadway grade while maintaining the same vertical profile, as demonstrated in

$$G(x) = 0.059628 + 3.32 \times 10^{-6} x - 3.79 \times 10^{-8} x^2 + 1.42 \times 10^{-11} x^3. \quad (17)$$

The regression equation also facilitated the solution of the Ordinary Differential Equation by ensuring that the grade function was continuous.

Here, x is the distance from the beginning of the test section (in meters), and $G(x)$ is the roadway grade (percent) at any location x.

B. Test Vehicles

Thirteen light-duty test vehicles were used in the study. These vehicles were selected to cover a wide range of light-duty vehicle combinations, as summarized in Table I. As indicated in the table, the selected vehicles represent a wide range of sizes and a variety of Environmental Protection Agency (EPA) vehicle classes.

TABLE I
SUMMARY OF LIGHT-DUTY TEST VEHICLE CHARACTERISTICS

Vehicle	P (kW)	η	Mass (kg)	m_{ta}/m (%)	A (m^2)	C_d	Throttle Level
1996 Geo Metro	41.0	0.65	1130	0.380	1.88	0.34	99%
1995 Acura Integra SE	105.9	0.68	1670	0.515	1.94	0.32	90%
1995 Saturn SL	92.5	0.72	1240	0.560	1.95	0.33	91%
2001 Mazda Protégé	97.0	0.70	1610	0.525	2.04	0.34	96%
2001 Plymouth Neon	98.5	0.75	1650	0.495	2.07	0.36	95%
1998 Ford Taurus	108.2	0.80	1970	0.575	2.26	0.30	88%
1998 Honda Accord	111.9	0.75	1770	0.610	2.12	0.34	91%
1995 BMW 740I	210.4	0.70	2370	0.515	2.27	0.32	94%
1995 Dodge Intrepid	120.1	0.68	2040	0.535	2.30	0.31	92%
1999 Ford CrownVic	149.2	0.70	2300	0.590	2.44	0.34	98%
1998 Ford Windstar	149.2	0.65	2270	0.550	2.73	0.40	91%
1995 Chevy S-10	145.5	0.72	1930	0.605	2.31	0.45	89%
1995 Chevy Blazer	145.5	0.65	2310	0.560	2.49	0.45	92%

Table I presents the main characteristics of each of the light-duty vehicles and related parameters for use in the powertrain model described earlier. Here is a description of each of the parameters listed in the table and how the values used in the study were obtained.

1) Vehicle engine power P (in kilowatts): The engine power was obtained from the vehicle specifications.
2) Efficiency $\boldsymbol{\eta}$: Power losses in the engine due to internal friction and other factors generally account for 5%–10% of the engine losses for light-duty vehicles [17]. We assumed the losses to be 6%. It should be noted that it does not refer the relationship (typically less than 35%) between the total energy contained in the fuel and the amount of energy used to perform useful work.
3) Vehicle mass, mass (in kilograms): Vehicle mass is an important parameter in the model as it determines the force required to accelerate a vehicle. Vehicle weights were conducted using General Electrodynamics Corporation weight scales with an advertised accuracy of 98%.
4) Percentage of vehicle mass on the tractive axle $\mathbf{m}_{\mathrm{ta}}/\mathbf{m}$ (in percent): Each axle was separately weighed. In the case of light-duty vehicles, typical values for front-wheel drive vehicles are in the range of 50%–65%, reflective of the high weight of the engine sitting on top of the axle. For rear-wheel drive vehicles, the mass on the tractive axle typically ranges between 35% and 50% of the total mass.
5) Frontal area $\mathbf{A}$ $(\mathbf{m}^2)$: The frontal area of the vehicle can be approximated as 85% of the height times the width of the vehicle if it was not directly given in the vehicle specifications.
6) Air drag coefficient $\mathbf{C_d}$: The air drag coefficient is given in the vehicle specifications. Typical values for light-duty vehicles range from 0.30 to 0.35, depending on the aerodynamic features of the vehicle. These values were also obtained from the vehicle specifications.
7) Throttle level: The throttle level was estimated by minimizing the deviation between the estimated and field observed speed trajectory, given that this information was not available. This is fine given that the intent of this testing effort is to establish the feasibility of the model in replicating field measurements.

C. Data Collection Procedures

Each of the test vehicles was subjected to the same set of tests. The test runs involved accelerating the vehicles from a complete stop at the maximum acceleration rate over the entire length of the 1.6-km test section from 0 km/h to the maximum attainable speed within the test section. Depending on the type of vehicle, maximum speeds attained by the end of the test section for light-duty vehicles varied between 128 and 160 km/h (80 and 100 mi/h) and was much lower for the heavy-duty trucks. In conducting the study, a minimum of five repetitions were executed for each test set to provide a sufficient sample size for the validation analysis.

In each test run, the speed and position of the vehicle was recorded using a portable GPS receiver connected to a laptop. Outputs from the GPS receiver included latitude, longitude, altitude, speed, heading, and time stamp once every second. Nominal position accuracy was specified with a 25-m (82-ft) spherical error probability, whereas nominal velocity accuracy was specified within 0.1-m/s (0.31-ft/s) error probability. Consequently, the error in acceleration estimates was within 0.1 m/s^2, given that they were computed every 2 s.

D. Roadway Parameters

To apply the vehicle dynamics model, five parameters linked to roadway characteristics must be determined: pavement type, pavement coefficient of friction, roadway grade, rolling coefficients, and altitude of roadway.

1) Pavement: The pavement type and condition are required to determine several parameters. As indicated earlier, the selected test section on the Smart Road facility had a Pavement Serviceability Index greater than 3.0 and thus was classified as "good." The pavement condition affects the coefficient of friction and rolling coefficients, as described in detail by Rakha *et al.* [18]. Consequently, a coefficient of friction of 0.8 and values of 1.25, 0.0328, and 4.575 were selected for the coefficients C_r, c_5, and c_6, respectively.
2) Grade: The roadway grade was computed using (17) at each vehicle position.
3) Altitude: This is the altitude above sea level for the testing location in meters. Since the Smart Road sits at an altitude of 600 m, this lead to determination of an altitude coefficient of 0.95, as described by Rakha *et al.* [18].

E. Testing Results

Using the roadway and vehicle parameters, the proposed model was used to compute the evolution of the vehicle powertrain parameters over time. Given that the level of throttle input provided by the driver (human-in-the-loop) was unknown, this parameter was optimized to minimize the sum of squared error (E) between the model and field observed speed and position predictions as

$$E = \frac{\sqrt{\sum_{t=0}^{T}(\hat{v}_t - v_t)^2}}{\overline{v}} + \frac{\sqrt{\sum_{t=0}^{T}(\hat{x}_t - x_t)^2}}{\overline{x}} \tag{18}$$

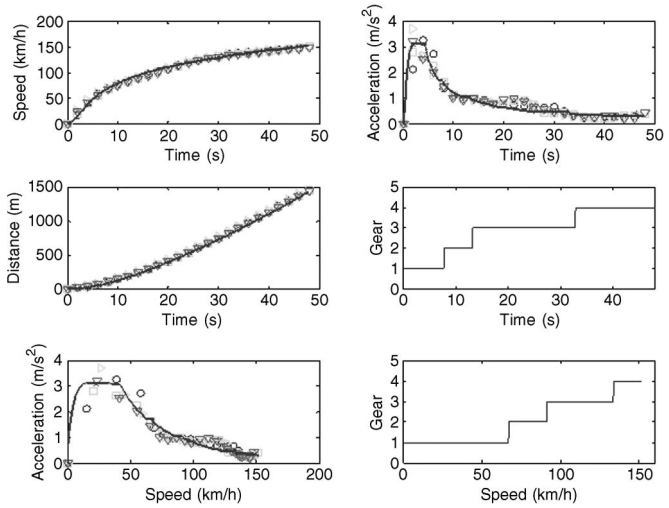

Fig. 3. Model validation against field measurements (Ford Crown Victoria).

where T is the total travel time (in seconds), hat variables ($\hat{}$) are model-estimated parameters, and nonhat variables are field observations. The sum of the squared error is normalized by dividing by the average field observed speed and distance traveled to ensure that the error is dimensionless.

The optimum throttle level values that were estimated for the 13 test vehicles, which are summarized in Table I, ranged from 55% to 92% with an average throttle level of 76% and a standard deviation of 14%. In capturing the vehicle behavior, Fig. 3 shows a good match between the model estimates and field measurements. The various symbols in the figure reflect the different runs that were executed on the test facility. The first of the subplots in the figure illustrates the variation in the vehicle speed as a function of the travel time. This figure clearly demonstrates a good match between the estimated and observed speed profiles. The second subplot compares the temporal variation in predicted vehicle acceleration levels against field observations. Again, the figure clearly demonstrates a good match between field and simulated behavior. The third subplot demonstrates an excellent match between the field-observed and model-estimated vehicle trajectories.

The proposed model estimates vehicle speed and distance with a margin of error of 11.9% when compared to field-measured GPS data for Ford Crown Victoria. The temporal variation in the transmission gear demonstrates that the vehicle travels in the first gear for approximately 8 s before upshifting to the second gear. The vehicle remains in the second gear for approximately 4 s before shifting to the third gear, and finally, the vehicle shifts to the fourth gear after 32 s.

Similar matches to the field data are observed for a compact vehicle (Mazda Protégé), as shown in Fig. 4, and a sports utility vehicle (Chevy Blazer), as shown in Fig. 5. Overall, the test vehicles estimated the vehicle speed, and accelerations within reasonable accuracy compared to the field-measured GPS data ranged from 13.4% to 16.8% errors. A comparison of the various vehicle behaviors demonstrates that larger vehicle engines are able to make gear shifts later in time and at higher speeds, whereas smaller engines require gear shifts at lower speeds.

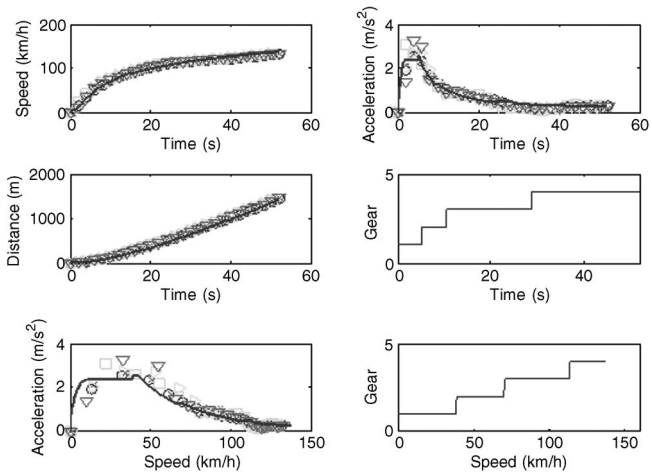

Fig. 4. Model validation against field measurements (Mazda Protege).

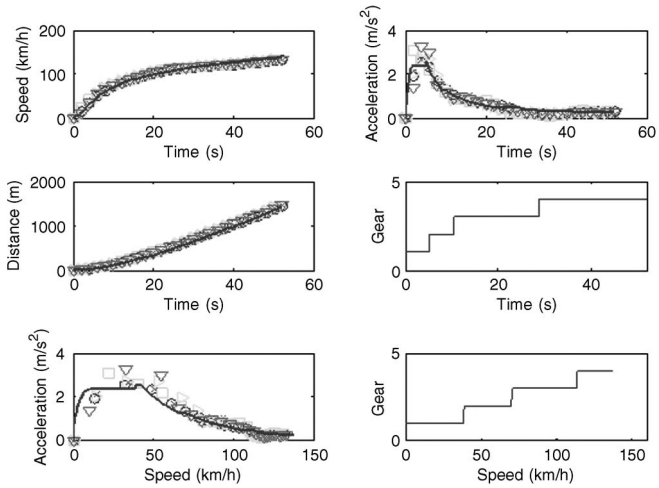

Fig. 5. Model validation against field measurements (Chevy Blazer).

IV. Model Validation

The second validation effort of the proposed powertrain model was conducted by comparing the model power and fuel consumption estimates to field-collected data along a 22-km section of Interstate 81. The 22-km section between mileposts 132 (Roanoke, VA) and 118 (Christiansburg, VA), which ranges from an elevation of 350 to 629 m above mean sea level was selected. For the southbound direction, significant grade sections exist with the need for two truck climbing lanes. The maximum grade along the study section is $+4\%$, the maximum downhill grade is -5% with an average grade of 0.6%, and more downhill grade sections are observed in the northbound direction. Both southbound and northbound trips were collected and analyzed for the study. The vehicle driving related data were collected using an OBD II data logger. The data included the instantaneous driver throttle input, fuel consumption, and speed.

The vehicle was driven using a cruise control system. The target speed was set to 104 km/h (or 65 mi/h). The input parameters to the model included only the vehicle parameters. The model then estimated the driver throttle input, the power used, and the fuel consumed. Figs. 6–8 show the measured

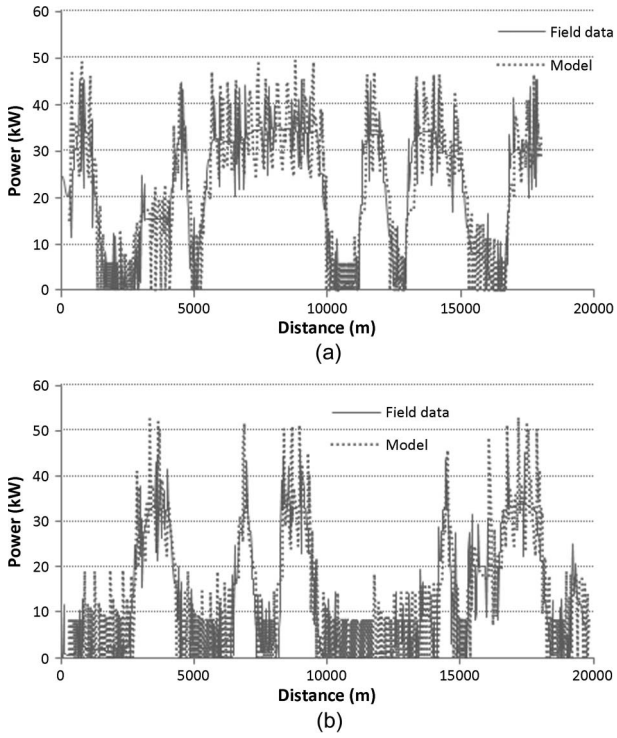

Fig. 6. Instantaneous model validation (2007 Chevy Malibu). (a) Interstate 81-Southbound. (b) Interstate 81-Northbound.

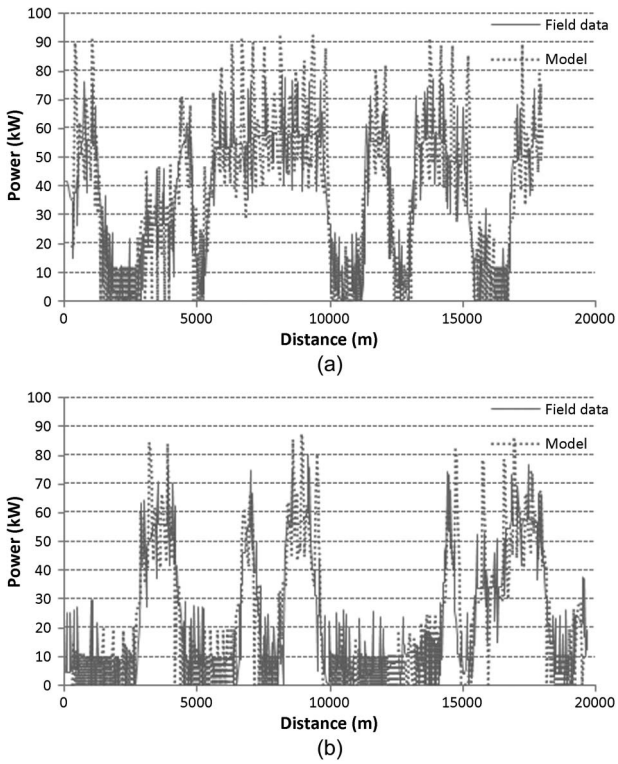

Fig. 7. Instantaneous model validation (2008 Chevy Tahoe). (a) Interstate 81-Southbound. (b) Interstate 81-Northbound.

instantaneous vehicle power exerted along the southbound and northbound section of Interstate 81 and the estimated power from the proposed model. The results clearly demonstrate a good agreement between the instantaneous power estimates and field measurements.

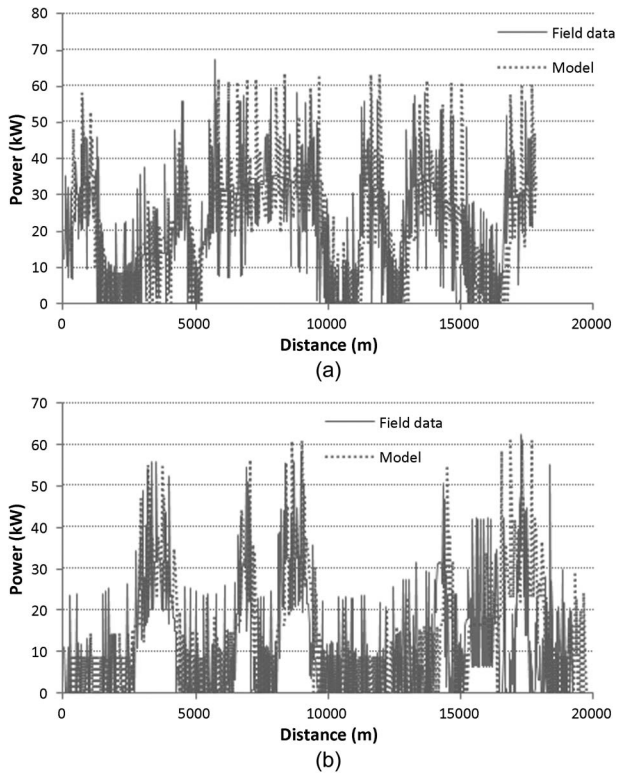

Fig. 8. Instantaneous model validation (2009 Toyota Camry). (a) Interstate 81-Southbound. (b) Interstate 81-Northbound.

Three test vehicles (Chevy Malibu, Chevy Tahoe, and Toyota Camry) were utilized for the validation study. As illustrated in the figures, the predicted power generally follows the peaks and valleys of the measured data, except for a few high power points. Specifically, 2007 Chevy Malibu generated 13 297 kW of power along the southbound section of Interstate 81, whereas the proposed model estimated a total of 13 871 kW of power using the same speed and road topographic profile, which is approximately a 4.3% error. Overall, the test vehicles estimated the vehicle power within a reasonable accuracy compared to the field-measured power data (error ranging between 1.7% and 20.2% for the three test vehicles).

Fig. 9 shows the power distributions of the model estimates and the field data for the southbound and northbound sections of Interstate 81 trips for the Chevy Malibu test vehicle. The figures illustrate a good fit between the model estimates and the field measurements. Specifically, the predictions typically follow the power distribution trend for both the southbound and northbound trips, except for a few cases. As shown in the figures, the southbound trips, which involve uphill grade sections, require more vehicle power than the northbound trips.

V. Vehicle Fuel Consumption Modeling

This section demonstrates how the proposed powertrain model is applied for vehicle fuel consumption modeling. In this section, the recently developed Virginia Tech Comprehensive Power-based Fuel Model (VT-CPFM) is utilized because it is easily calibrated using publicly available fuel economy data

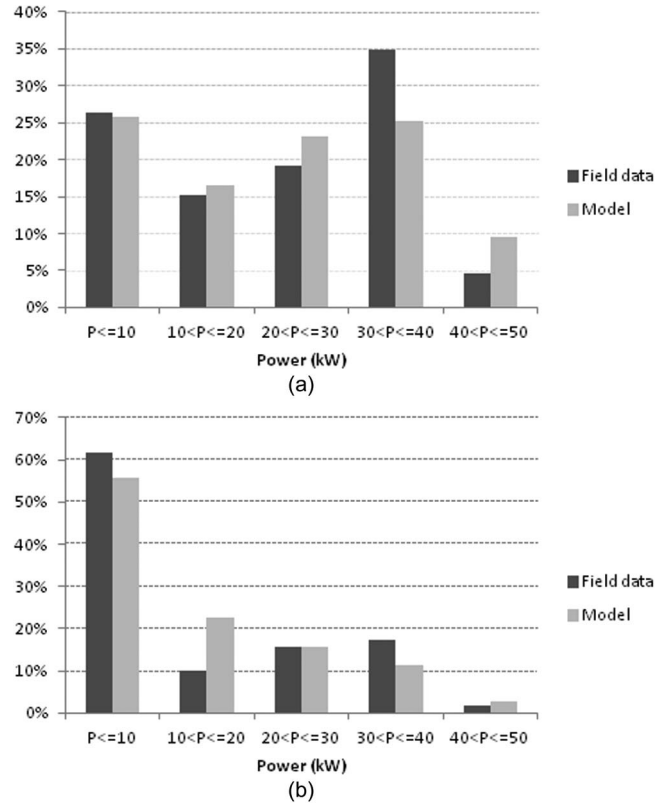

Fig. 9. Power distribution (2007 Chevy Malibu). (a) Interstate 81-Southbound. (b) Interstate 81-Northbound.

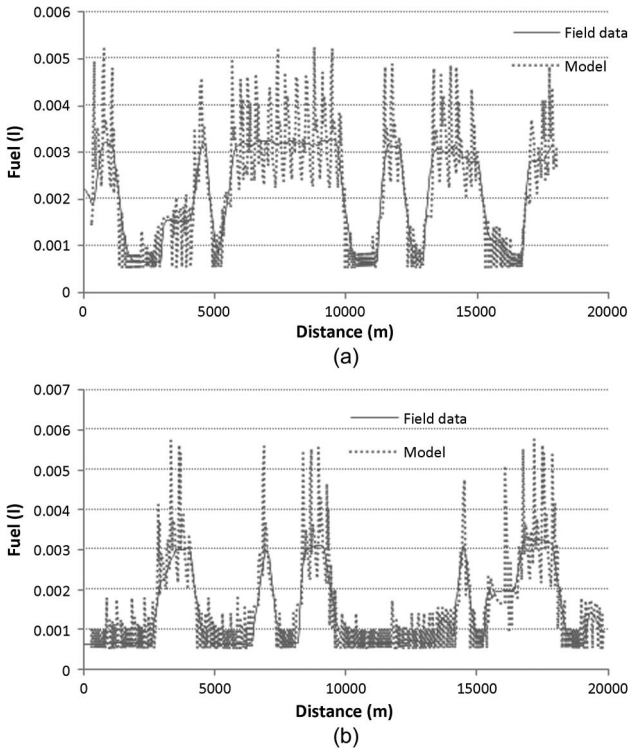

Fig. 10. Fuel consumption validation (2007 Chevy Malibu). (a) Interstate 81-Southbound. (b) Interstate 81-Northbound.

that are rated by the U.S. EPA. There are two models that are formulated as

$$FC(t) = \alpha_0 + \alpha_1 P(t) + \alpha_2 P(t)^2 \tag{19}$$

$$FC(t) = \beta_0 \omega_e + \beta_1 P(t) + \beta_2 P(t)^2 \tag{20}$$

where $FC(t)$ is the vehicle fuel consumption rate (in liters per second) at instant t; α_0, α_1, α_2, β_0, β_1, and β_2 are model constants that require calibration; $P(t)$ is the instantaneous total power in kilowatts at instant t; and $\omega(t)$ is the engine speed at instant t. If the power is negative, it is set to zero. A detailed description of the fuel consumption model and the validation of the model are described in the literature [19].

The instantaneous measured and estimated fuel consumption rates were compared by simulating the test vehicle (2007 Chevy Malibu) on the southbound and northbound study sections of Interstate 81, as shown in Fig. 10. Superimposed on the figures are the fuel consumption model (VT-CPFM-1 model) estimates, which were computed using the vehicle-specific parameters. The figure indicates a close match between predicted and measured fuel consumption levels and demonstrates a good agreement with field measurements. While it appears that the proposed model overestimates and underestimates some fuel consumption rates, in general, the model predictions follow the field-collected fuel measurements. Specifically, in the case of the southbound trip, the test vehicle consumed 1.33 L of fuel, whereas the model estimated 1.40 L of fuel, which is a margin of error of 5.5%. In addition, the test vehicle used 0.96 L of fuel for the northbound trip, whereas the model estimated 1.08 L of gasoline, which is approximately 12.8% of error.

VI. Conclusion

The research presented in this paper has developed a simple vehicle powertrain model that can be integrated with car-following models within microscopic traffic simulation software. This simple model can be calibrated using engine and powertrain parameters that are publicly available without the need for field data collection. The model uses the driver throttle level input to compute the engine speed; model the transmission system (manual and automatic); and finally compute the vehicle's acceleration, speed, position, and fuel consumption level. The model has demonstrated to produce vehicle acceleration, speed, position, and fuel consumption estimates that are consistent with field observations.

References

[1] B. K. Powell, "A dynamic model for automotive engine control analysis," in *Proc. 18th IEEE Conf. Decision Control*, 1979, pp. 120–126.

[2] J. D. Powell, "A review of IC engine models for control system design," in *Proc. 10th IFAC World Congress.*, Munich, Germany, Jul. 1987, vol. 3.

[3] D. J. Dobner, "A mathematical engine model for development of dynamic engine control," Soc. Autom. Eng., Warrendale, PA, SAE Tech. Paper 800054, 1980.

[4] J. J. Moskwa and J. K. Hedrick, "Automotive engine modeling for real time control application," in *Proc. Amer. Control Conf.*, Minneapolis, MN, 1987, pp. 241, 341–346.

[5] P. Yoon and M. Sunwoo, "A nonlinear dynamic modelling of SI engines for controller design," *Int. J. Veh. Des.*, vol. 26, no. 2/3, pp. 277–297, 2001.

[6] D. Cho and J. K. Hedrick, "Automotive powertrain modeling for control," *Trans. ASME, J. Dyn. Syst. Meas. Control*, vol. 111, no. 4, pp. 568–576, Dec. 1989.

[7] L. Guzzella and A. Sciarretta, *Vehicle Propulsion Systems—Introduction to Modeling and Optimization*., 2nd ed. New York: Springer-Verlag, 2007.

[8] U. Kiencke and L. Nielsen, *Automotive Control Systems: For Engine, Driveline, and Vehicle*., 2nd ed. Berlin, Germany: Springer-Verlag, 2005.
[9] D. Ni and D. Henclewood, "Simple engine models for VII-enabled in-vehicle applications," *IEEE Trans. Veh. Technol.*, vol. 57, no. 5, pp. 2695–2702, Sep. 2008.
[10] H. Rakha, P. Pasumarthy, and S. Adjerid, "A simplified behavioral vehicle longitudinal motion model," *Transp. Lett., Int. J. Transp. Res.*, vol. 1, no. 2, pp. 95–110, Apr. 2009.
[11] H. Rakha, P. Pasumarthy, and S. Adjerid, "Modeling longitudinal vehicle motion: Issues and proposed solutions," in *Proc. Transp. Sci. Technol. Congr.*, Athens, Greece, 2004, p. [PAN103].
[12] H. Rakha, M. Snare, and F. Dion, "Vehicle dynamics model for estimating maximum light-duty vehicle acceleration levels," *Transp. Res. Rec.*, vol. 1883, no. 1, pp. 40–49, 2004.
[13] H. Rakha and I. Lucic, "Variable power vehicle dynamics model for estimating maximum truck acceleration levels," *J. Transp. Eng.*, vol. 128, no. 5, pp. 412–419, Sep./Oct. 2002.
[14] E. Hellstrom, "Explicit use of road topography for model predictive cruise control in heavy trucks," M.S. thesis, Elect. Eng., Linköpings Univ., Linköping, Sweden, 2005.
[15] G. Genta, *Motor Vehicle Dynamics: Modeling and Simulation*. Singapore: World Scientific, 2003.
[16] M. D. Artamonov, V. A. Ilarionov, and M. M. Morin, *Motor Vehicles: Fundamentals and Design*. Moscow, Russia: Mir Publisher, 1976.
[17] J. Y. Wong, *Theory of Ground Vehicles*., 3rd ed. New York: Wiley, 2001.
[18] H. Rakha, I. Lucic, S. H. Demarchi, J. R. Setti, and M. Van Aerde, "Vehicle dynamics model for predicting maximum truck acceleration levels," *J. Transp. Eng.*, vol. 127, no. 5, pp. 418–425, Sep./Oct. 2001.
[19] H. Rakha, K. Ahn, K. Moran, B. Saerens, and E.V.D. Bulck, "Virginia tech comprehensive power-based fuel consumption model: Model development and testing," *Transp. Res. Part D, Transp. Environ.*, vol. 16, no. 7, pp. 492–503, Mar. 2012.

Hesham A. Rakha (M'04) received the B.Sc. degree (with honors) in civil engineering from Cairo University, Cairo, Egypt, in 1987 and the M.Sc. and Ph.D. degrees in civil and environmental engineering from Queen's University, Kingston, ON, Canada, in 1990 and 1993, respectively.

He is currently a Professor with the Charles E. Via, Jr. Department of Civil and Environmental Engineering, Virginia Tech, Blacksburg, and the Director of the Center for Sustainable Mobility, Virginia Tech Transportation Institute. He has authored/coauthored more than 210 refereed publications, of which 97 are fully refereed journal publications. His research interests include traffic flow theory, traffic modeling and simulation, dynamic traffic assignment, traffic control, energy and environmental modeling, and safety modeling.

Dr. Rakha is a member of the Institute of Transportation Engineers, the American Society of Civil Engineers, and the Transportation Research Board. He is a Professional Engineer in Ontario.

Kyoungho Ahn received the Ph.D. degree in civil and environmental engineering from Virginia Tech, Blacksburg, in 2002.

He is currently a Senior Research Associate with the Center for Sustainable Mobility, Virginia Tech Transportation Institute. He has developed and conducted extensive research as a Coprincipal Investigator and Faculty Investigator in vehicle energy and environmental modeling, traffic simulation, traffic flow theory and modeling, environmental impacts on transportation systems, intelligent transportation systems, advanced traffic signal control systems, and traffic impact studies. He has authored or coauthored more than 50 refereed publications, of which 15 are fully refereed journal publications.

Waleed Faris received the B.Sc. degree in mechanical engineering with a specialization in construction equipment and off-road vehicles and the M.Sc. degree in applied mechanics from Zagazig University, Zagazig, Egypt, in 1989 and 1996, respectively, and the Ph.D. degree in nonlinear dynamics from Virginia Tech, Blacksburg, in 2003.

He is currently the Deputy Dean of the Corporate Strategy and Quality Assurance Office, International Islamic University Malaysia, Kuala Lumpur, Malaysia, and has been an Associate Professor with the Department of Mechanical Engineering and Department of Mechatronics since 2004. He has to his credit three books and more than 80 technical papers in reputed journals and refereed conference proceedings in vehicle, structural, and system dynamics and control and Noise, Vibration, and Harshness (NVH).

Dr. Faris is a member of the Japanese Society of Automotive Engineers and a technical committee member and reviewer of several international journals and conferences worldwide.

Kevin S. Moran received the B.Sc. degree in mechanical engineering from the University of Michigan, Ann Arbor, in 1977

He is currently the Director of Global Products with Advanced Driver Assistance Systems, NAVTEQ Corporation, Chicago, IL. He is executing NAVTEQ's initiative in advanced driver assistance systems (ADASs) and is responsible for defining market requirements and driving business for digital map-enhanced ADAS applications. In this role, he focuses on lead market opportunities, as well as demonstrating the technical benefits of digital maps to ADASs. Prior to NAVTEQ, he was with Spotwave Wireless, leading the development and market launch of mobile wireless signal enhancement technologies, and with Motorola, where he was the Director of the Telematics Communications Group. In this role, he launched first-and next-generation Telematics products in North America, Europe, and Japan; directed business strategy; and created advanced Infotainment solutions. Earlier at Motorola, he launched groundbreaking automotive emission controls and sensors.